Parsimonious Methodology for Synthesis of Silver and Copper Functionalized Cellulose

David Patch (david.patch@rmc.ca)
Royal Military College of Canada
Natalia O'Connor
Royal Military College of Canada
Debora Meira
Royal Military College of Canada
Jennifer Scott
Royal Military College of Canada
Iris Koch
Royal Military College of Canada
Kela Weber
Royal Military College of Canada

Research Article

Keywords: Cellulose ,Silver nanomaterials , Copper nanomaterials ,Green synthesis ,In-situ synthesis

Posted Date: July 5th, 2022

DOI: https://doi.org/10.21203/rs.3.rs-1793366/v1

Additional Declarations: No competing interests reported.

Version of Record: A version of this preprint was published at Cellulose on February 25th, 2023. See the published version at https://doi.org/10.1007/s10570-023-05099-7.

Abstract

Metal nanomaterials, such as silver and copper, are often incorporated into commercial textiles to take advantage of their antibacterial and antiviral properties. In this study eight different methods were employed to synthesize silver, copper, and silver/copper functionalized cotton batting textiles. Using silver and copper nitrate as precursors, different reagents were used to initiate/catalyze the deposition of metal, including: (1) no additive, (2) sodium bicarbonate, (3) green tea, (4) sodium hydroxide, (5) ammonia, (6,7) sodium hydroxide/ammonia at a 1:2 and 1:4 ratio, and (8) sodium borohydride. The use of sodium bicarbonate as a reagent to reduce silver onto cotton has not been used previously in literature and was compared to established methods. All synthesis methods were performed at 80˚C for one hour following textile addition to the solutions. The products were characterized by X-ray fluorescence (XRF) analysis for quantitative determination of the metal content and X-ray absorption near edge structure (XANES) analysis for silver and copper speciation on the textile. Scanning electron microscopy (SEM) with energy dispersive X-ray (EDX) and size distribution inductively coupled plasma mass spectrometry (ICP-MS) were used to further characterize the products of the sodium bicarbonate, sodium hydroxide, and sodium borohydride synthesis methods following ashing of the textile. For the silver treatment methods (1 mM Ag+), sodium bicarbonate and sodium hydroxide resulted in the highest amounts of silver on the textile (8900 mg Ag/kg textile and 7600 mg Ag/kg textile) and for copper treatment (1 mM Cu+) the sodium hydroxide and sodium hydroxide/ammonium hydroxide resulted in the highest amounts of copper on the textile (3800 mg Ag/kg textile and 2500 mg Ag/kg textile). Formation of copper oxide was dependent on the pH of the solution, with 4 mM ammonia and other high pH solutions resulting in majority of the copper on the textile existing as copper oxide, with smaller amounts of ionic-bound copper.

1. Introduction

Metals such as silver and copper have been used in medical, religious, and ornamental applications for thousands of years [1, 2]. Many of these applications used bulk metals, such as silver containers for water purification, or ionic salts, such as silver nitrate as a caustic for wound treatment [3]. Advances in material sciences have seen the synthesis of smaller and smaller metal materials, seeking to taking advantage of the increased surface area to volume ratio and the unique properties these metals have compared to the larger bulk counterparts. These materials are often classified according to their size, with fine particles (2,500–100 nm), nanoparticles (100–1 nm), and atom clusters (< 1 nm) being the three smallest ranges. The definition of nanoparticles is sometimes expanded to include particles 500 nm and smaller, since these particles still exhibit some nanoscale properties [4–7].

Metal nanoparticles and nanocomposites are a growing focus of commercialization because of the beneficial qualities these nanomaterials can impart. One of the biggest areas of growth is in the development of nano-functionalized textiles with manufacturers seeking to take advantage of the antibacterial properties of the nanomaterials. Metal and metal oxide nanoparticles are often utilized as these have enhanced stability and antibacterial efficacy over other oxidation states. Silver is often selected for antibacterial applications, and copper is selected for antiviral and antifungal applications.

Silver and copper are the most commonly studied metals used for creating high performance textiles (Figure S1). The COVID-19 pandemic has renewed interest in using nanotechnology for enhanced protectiveness against viral spread [8]. Other than antimicrobial activity, nanoparticles can impart unique properties to textiles including increased conductivity[9, 10], self-cleaning[11], electromagnetic interference shielding [12] and ultraviolet shielding[13].

There are two common ways to prepare textiles with nanoparticles: ex-situ and in-situ. The ex-situ approach involves first forming metal nanoparticles separately from the textile, using a wet chemical method [14–16], a sacrificial anode method (Ditaranto et al., 2016), or a biological method[18–20]. The particles formed ex-situ are then applied to textiles through immersion or dry padding [21]. The in-situ approach consists of synthesizing nanoparticles directly onto the textiles, using an electroless plating or a chemical reduction method [22–25]. Some of these in-situ methods use an added reducing agent (e.g., glucose)[26] or use the textile polymer itself (e.g., cellulose in cotton textiles) as the reducing agent [27–29]. Cellulose is the most popular textile polymer used, due to its aesthetic qualities as well as it being renewable and biocompatible (Figure S1) [30, 31].

The electron rich functional groups and polymer structure of cellulose allows for initial complexation of the ionic metal and stabilization of the resultant metal nanoparticle [32]. The extent of deposition, speciation, and morphology of the resultant metal nanoparticle is heavily influenced by the synthesis conditions, including heat, pH, and reagents used [13, 25, 33–36]. To the knowledge of the authors, there have been no previous studies quantitatively characterizing the concentration, speciation, and morphology of the resultant metal materials across different synthesis methods.

The goal of the present study is to identify a parsimonious synthesis method for creating silver, copper, and bimetallic treated textiles by comparing eight different synthesis methods. A selection of novel and popular synthesis methods are examined through a stepwise approach. The parsimony of the synthesis method are evaluated based on three criteria: high metal content, measured by x-ray fluorescence spectroscopy (XRF); metallic or metal-oxide speciation, determined using x-ray absorption near-edge structure (XANES); and consistent particle morphology, determined using scanning electron microscopy (SEM).

2. Materials And Methods

2.1 Reagents

Silver nitrate (ACS), copper (II) nitrate hemipentahydrate (ACS), sodium hydroxide pellets (ACS), ammonia solution (28–30%, ACS), sodium bicarbonate (ACS), Triton X100, and sodium borohydride (ACS) were all purchased from VWR. Cotton batting was purchased from a local supplier in Kingston, Ontario (Stitch by Stitch). Green tea was purchased from a local grocery store (Metro). Deionized water (DI water) was generated using an in-lab filtration system (Milli-Q Direct 8, 18 MΩ).

2.2 Preparation

All glassware was cleaned three times with 2% nitric acid and then rinsed with three portions of DI water. 4x4 cm squares of cotton batting (106 g/m^2) were cut from the bulk material using a rotary cutter and prepared as follows: (1) washed with 1% Triton X100 solution at 60°C for 30 minutes with agitation (2) rinsed with DI water until no foaming was observed, (3) rinsed with DI water at 60°C for 15 minutes with agitation; and (4) dried overnight in an oven at 40°C. Textiles were trimmed with a rotary cutter after drying to remove any stray strands of batting.

2.3 Synthesis

A summary of the methods and reagents used is provided in Table 1, with a general procedure described in the following paragraphs. A final volume of 13.6 mL of solution and 0.17 ± 0.01 g of cotton batting was used to obtain a volume/textile mass ratio of 80:1, to allow for thorough wetting and mixing of the solutions. Erlenmeyer flasks were filled with DI water, sealed with aluminum foil, and placed into a water bath (digital general water bath, VWR) set to 60°C. Reagents were added as appropriate for each method, shown in Table 1, and agitated for 10 minutes using an orbital shaker.

Table 1
Overall synthesis steps performed, including reagents added at each step and analytical methods employed.

Method #	1	2	3	4	5	6	7	8
Short name	Control	$NaHCO_3$	$NaHCO_3$ + green tea	NH_3	NaOH	NaOH/ $NH_{3Version1}$	NaOH/ $NH_{3Version2}$	$NaBH_4$
Step 1: Reagents added and mixed at 60°C for 10 minutes								
Step 1 reagents	DI H_2O	4 mM $NaHCO_3$	4 mM $NaHCO_3$	4 mM NH_3	4 mM NaOH	2 mM NaOH + 4 mm NH_3	2 mM NaOH + 8 mm NH_3	DI H_2O
Step 2: Metals added and mixed at 60°C for 10 minutes								
Step 2 metals	1 mM Ag^+ OR 1 mM Cu^+ OR [0.5 mM Ag^+ + 0.5 mM Cu^+]							
Step 3: Textile added, temperature set to 80°C								
Step 4: Reagents added								
Step 4 reagents	none	none	1% green tea	none	none	none	none	4 mM $NaBH_4$
Step 5: Mixed at 80°C for 1 hour								
Step 6: Cooled, drained, textile rinsed with DI H_2O at least 3x, and dried at 60°C overnight								
Step 7: Textiles characterized using methods listed below								
XRF	x	x	x	x	x	x	x	x
XANES	x	x	x	x	x	x	x	x
ATR-FTIR		x			x	x		x
SEM/EDX		x			x			x
ISE		x (Ag)						

Silver and/or copper nitrate solutions were added to the flasks to reach the final concentrations listed in Table 1 and mixed for 10 minutes. One textile (4 x 4 cm, 0.17 ± 0.01 g) was added to each Erlenmeyer flask, the water bath temperature was raised to 80°C, and reagents were added for Methods 3 and 8 (see Table 1). Flasks were agitated on an orbital shaker at 30 RPM for one hour. The Erlenmeyer flasks were then removed from the shaker, and 12 mL of room temperature DI water was immediately added to cool the vessel and stop the reaction. The following steps were untaken to process the textiles: (1) textiles were removed from the solutions and rinsed with 20 mL DI water three times, (2) additional rinses were

performed, if necessary, until the rinse solution was clear (e.g., for Method 2) (3) water was gently squeezed from the textiles, and (4) textiles were dried at 60^0C in an oven overnight. Synthesis methods were performed in triplicate. A digital camera (Canon SL2) was used to image the textiles after the synthesis reactions to record color change.

Additional experiments were performed to explore the effect of heat, silver/copper competition, and for cellulose analysis. These experiments were performed using synthesis method 6 as it is a well-established method in literature.

2.4 Metal Content Determination

The metal concentration of the textiles following treatment was measured using x-ray fluorescence spectroscopy (Innov-X Systems α-2000 XRF). Textiles were analyzed whole after drying and the concentration determined by using an external calibration curve, since the XRF measurement parameters were set up for soil samples and not applicable to textiles. (See SI for method development of this calibration). Two calibration curve preparation methods were explored to determine the more accurate method. XRF detection limits were identified as ~ 375 mg Ag/kg and ~ 100 mg Cu/kg. Relative standard deviation for replicates was found to be 16 ± 11%.

2.6 Metal Speciation

X-ray absorption near edge structure (XANES) analysis was used to perform silver and copper speciation analysis of the bulk textiles. XANES spectra were collected at the Sector 20 insertion device beamline (20ID-C) of the Advanced Photon Source (CLS@APS), within the X-Ray Science Division (XSD), Argonne National Laboratory. XANES spectra of the Ag Kα-edge and Cu Kα-edge were recorded in fluorescence mode by using a four-element silicon drift detector (Vortex®-ME4 with Xspress 3 pulse processor) while monitoring incident and transmitted intensities in straight ion chamber detectors filled with N_2 gas. Textiles were analyzed as 1cm x 1cm subsections rolled and packed in a 3D printed PETG sample holder, held between two layers of Kapton® tape. The Si (111) double crystal monochromator was calibrated using a silver metal foil at 25,514 eV, copper metal foil at 8989 eV, and the incident beam size was 800 µm. Fitting of XANES spectra was accomplished with Athena software. The silver standard spectra used for fitting had been measured as frozen aqueous dissolved species previously by our group[37], and included AgNP, $AgNO_3$, AgO. The copper standards were synthesized in our lab using copper nitrate as a precursor and reacting it with the appropriate reagents to form the desired precipitate (where applicable). After synthesis, standards were washed with three portions of DI water and packed into the same 3D printed sample holder. The Ag (0) and Cu (0) standards used provided the metals in their zero oxidation state and could not distinguish between nanoparticulate or bulk metallic forms.

2.7 Metal Morphology

Complete SEM sample preparation development is described in detail in the SI. Initial SEM analysis of the textiles failed to identify substantial metal materials on the textile surface, despite high concentrations present on the textiles (Figure S3). Cross-sectional analysis of the textiles identified the presence of

nanomaterials within the cotton fiber core itself (Fig. 1). This led to the development of a textile ashing method that allowed for improved metal morphological determination.

Separate square subsections of the textiles (approximately 0.1 g) were ashed in ceramic crucibles at 550°C for one hour [38]. The resulting grey ash was dispersed in 1 mL DI water, and diluted to 10 mL with DI water, ultrasonicating the solution at 30 kHz for one minute. A 0.1 mL subsample of the solution was dried onto double-sided carbon tape and analyzed. Surface analysis of the textile samples were analyzed (Quanta 250FED) operating under environmental mode at 100 kPa. EDX (EDAX Octane Elite) was performed for elemental determination. Analysis of the dried ash following reconstitution were analyzed on under high vacuum mode. Images were acquired first at 6000–7500 magnification, then taken at 18–21,000 magnification. ImageJ (NIH) was used to count and determine the spherical diameter for nanoparticles. For non-spherical or oval nanoparticles, the diameter was measured at the shortest dimension.

2.8 Fourier-Transform Infrared Spectroscopy (FTIR) Analysis

The FTIR (Thermo Scientific Nicolet-IS10 Attenuated Total Reflection (ATR)-FTIR) spectra of cotton samples were acquired by folding samples twice for a total of four layers before being placed into the active element of the ATR-FTIR.

2.9 Ion Selective Electrode (ISE) Analysis

Using a silver ion selective electrode (Fisher Scientific accumet), the kinetics of the $NaHCO_3$ synthesis method were explored at temperature profile 1 (60°C heated to 80°C) and temperature profile 2 (80°C from the start) by measuring the decrease in ionic silver present in the solution (assumed to correspond to formation of particulate silver on the textile). It is important to note that, as the ISE only measures ionic silver, any release of metallic silver from the textile during synthesis would not be identified. A no-textile control was analyzed using ISE at both temperature profiles to correct for changes to ISE response as a function of temperature. A six-point external calibration curve at the reaction temperature was used to quantify the ionic silver.

3. Results And Discussion

3.1 Metal Content and Speciation on Textile

Visual inspection of the treated cellulose textiles (see Fig. 2) allowed for an immediate indication of the effectiveness of the different synthesis methods. Based on the extent of discoloration, the silver synthesis reactions with $NaHCO_3$, NaOH, or $NaOH/NH_{3Version1}$ (Methods 2, 4 and 5) resulted in substantial silver present on the textile (darker brown), whereas copper synthesis methods 4, 5, 6, 7 and 8 appeared to have the most copper present (Fig. 2). With the combined silver/copper treatment methods,

the color trend of the textiles is similar to either their silver or copper textile counterpart, indicating a likely dominance of silver (method 2) or copper (methods 4–8).

XRF analysis confirms some of the observations made from the textile images: for the separate silver and copper textiles, the use of $NaHCO_3$, NaOH and $NaOH/NH_{3Version1}$ (Methods 2, 4 and 5) resulted in the highest amounts of silver (Fig. 3A, S5), and methods 4–8 resulted in comparably high amounts of copper on the textile (Fig. 3B, S5). For silver/copper bimetallic treatment, the use of $NaHCO_3$ (Method 2) resulted in highest amount of silver, but methods 4–7 resulted in reduced silver concentrations and copper dominating (Fig. 3C, S5).

XANES analysis identified the metal speciation of silver and copper across the synthetic trials. For silver only synthetic trials, all the methods resulted in reduction of the ionic silver into metallic silver (Fig. 3a).

It is well accepted that ionic metals, such as silver, can be reduced by cellulose in cotton, and this reduction occurs more completely under alkaline conditions and at elevated temperatures [39–41]. The exact mechanism of this reduction is not often discussed in detail although some authors suggest that the hydroxyl groups on the cellulose polymer are oxidized into aldehydes, and then into carboxylates [42]. However, silver complexes like those formed using Tollen's Reagent are not reduced in the presence of alcohol-containing compounds in classic chemical tests, whereas they are with aldehydes. Other authors identify that while cellulose itself is not considered a reducing sugar; hemiacetal groups are present at the termini of the polymer chain. These hemiacetals undergo ring-chain tautomerism under basic conditions and with heat (8), converting into aldehyde groups that, like typical reducing sugars such as glucose, can reduce metals [43–45]. There is also the potential for alkaline degradation of the cellulose polymer (i.e., the Lobry de Bruyn-Alberda van Ekenstein transformation[46]), resulting in the generation of glucose and other monosaccharides that will readily reduce ionic silver. It is also possible that the pectins and hemicelluloses present in the primary wall and winding layer of cotton fibers are reducing ionic silver, as these compounds have been found to reduce silver when isolated and used as primary reagents [47, 48].

When no reagents are added, as is the case with the positive control synthesis method, some reduction of silver is observed to be occurring (as detected by XANES). Reduction of ionic silver onto cotton without the use of reagents has been observed previously, with the concentration of silver being related to reaction time and temperature [34, 49].

The reactions for silver explored in this study are shown in equations 1 to 9 below. It is important to note that the silver hydroxide (3) immediately reacts to silver oxide (4) due to the favorable kinetics of the reaction (pK = 2.88) [50] (4). The silver complex formed following addition of NaOH and NH_3 (method 6, 7) is known as Tollen's reagent, which is used to test for aldehydes and alpha-hydroxy ketones and is often used for synthesizing silver-treated textiles [41, 42]. Reaction of the silver compounds with the aldehyde at the terminal end of the cellulose chain results in reduction of ionic silver to metallic silver, and oxidation of the aldehyde to the carboxylic acid.

If NaHCO3 is added

$$2Ag^{+} + HCO_3^{-} \rightarrow Ag_2CO_3 + H^{+} \quad (1)$$

If only NH_3 is added

$$Ag^{+} + 2NH_3 \rightarrow [Ag\ (NH_3)_2]^{+} \quad (2)$$

If only NaOH

$$Ag^{+} + OH^{-} \rightarrow AgOH \quad (3)$$

$$2AgOH \rightarrow Ag_2O + H_2O \quad (4)$$

If NH_3 and NaOH are added

$$Ag^{+} + OH^{-} \rightarrow AgOH \quad (5)$$

$$2AgOH \rightarrow Ag_2O + H_2O \quad (6)$$

$$Ag_2O + 4NH_3 + 2OH^{-} \rightarrow 2[Ag\ (NH_3)_2]OH \quad (7)$$

Hemiacetal cellulose ring chain tautomerism in the presence of base/heat

$$C_5H_7O_4\text{-}CH_3\text{-}OH \rightleftharpoons C_5H_7O_4\text{-}CH_2{=}O \quad (8)$$

Upon addition of cotton textile

$$Ag^{(+1)}Complex + C_5H_7O_4\text{-}CH_2{=}O \rightarrow Ag^{0} + C_5H_7O_4\text{-}COO^{-} \quad (9)$$

The resulting silver nanoparticles (8) are then stabilized by the cellulose inside the cotton fibers, similar to the stabilization effect that occurs with carboxymethylcellulose (CMC) coated nanoparticles [41, 51, 52].

While the speciation of silver on the textile was consistent across the methods, the amount of metal present on the textile varied substantially. This can be explained by the stability of the silver compounds. In the presence of green tea, reduction followed by stabilization via coating occurs, significantly inhibiting any silver deposition onto textile [53–58]. In the presence of ammonia (method 4), or high concentrations of ammonia (method 7) significant silver-ammonia complexation occurs, which stabilizes the silver and makes it a weaker oxidizing agent than the corresponding aquo complexes that result with Ag_2O and Ag_2CO_3. When $NaBH_4$ was added reduction occurred in the solution (a process well understood in literature)[59–66], causing the majority of silver nanomaterials to aggregate and precipitate out of solution before they could be deposited and stabilized by the cellulose (10).

$$2Ag^{+1} + 2BH_4^{-1} \rightarrow 2Ag + H_2 + B_2H_6 \quad (10)$$

For copper only synthetic trials, methods 1–3 resulted in the copper being deposited as ionic copper; likely intermolecularly bonded with the hydroxyl groups in the cellulose chain. For methods 4–7, which occurred at higher pH (pH > 10), the copper was deposited mainly as copper oxide. The reactions for copper explored in this study are shown in equations 11 to 17. When both NaOH and NH_3 are added, a copper-tetraammine-hydroxide complex is eventually formed, similar to the complex known as Schweizer's reagent, which is copper ammonia complex used to dissolve cellulose (14,15). Despite the various complexes that are formed, all of the pH > 10 complexes are not stable at elevated temperatures and convert into copper oxide, supporting the speciation results observed [67].

If only $NaHCO_3$ is added

$$Cu^{+2} + HCO_3^{-} \rightarrow Cu_2(OH)_2CO_3 \quad (11)$$

If only NH_3 is added

$$Cu^{+2} + NH_3 \rightarrow [Cu(NH_3)_4]^{+} \quad (12)$$

If only NaOH

$$Cu^{+2} + 2OH^{-} \rightarrow Cu(OH)_2 \quad (13)$$

If NH_3 and NaOH are added

$$Cu^{+2} + 2OH^{-} \rightarrow Cu(OH)_2 \quad (14)$$

$$Cu(OH)_2 + 4NH_3 \rightarrow [Cu(NH_3)_4](OH)_2 \quad (15)$$

In the presence of heat

$$Cu^{(+2)}\text{Complex (pH} > 10) \rightarrow CuO \quad (16)$$

The use of $NaHCO_3$ and $NaHCO_3$/green tea did not have any appreciable effect on the total concentration or speciation of copper on the textile when compared to the reagent-free control, indicating these reagents are superfluous for copper textile synthesis. This was initially unexpected as the antioxidants in green tea have been shown capable of reducing other metals like iron and silver. It is likely the $NaHCO_3$ precipitated out the ionic copper as copper (II) carbonate before reduction with green tea could occur.

When ionic copper and sodium borohydride react, the initial reduction follows a slightly different path when compared to the ionic silver reduction mechanism. In this reaction, ionic copper reacts with the sodium borohydride to form the reduced copper, hydrogen gas, and boric acid (17)[61].

$$2Cu^{+2} + 4BH_4^{-1} + 12H_2O \rightarrow 2Cu + 14H_2 + 4B(OH)_3 \quad (17)$$

The speciation of copper using $NaBH_4$ was expected to be metallic copper, based on $NaBH_4$ being a strong reducing agent, instead of the copper oxide that was found. It is hypothesized that copper treated

onto the textile underwent oxidation during drying and storage in ambient atmosphere, resulting in the formation of copper oxide.

XANES analysis for the bimetallic textiles identified a significant amount of ionic silver for methods 4–7, which was not present for the silver-only synthetic trials. Given the chemistry of copper oxide formation for methods 4–7, this incomplete reduction is likely due to copper partially outcompeting silver for binding onto the textile.

Due to the novelty of the $NaHCO_3$ method and the unexpected results additional experiments were performed to investigate the kinetics of reaction as a function of temperature profiles (Fig. 4), and the final textile concentration as a function of pH (Figure S6).

The reduction of silver by cellulose with $NaHCO_3$ is directly affected by the temperature of the reaction. As temperature is shifted from 60°C to 80°C, the rate of silver reduction increases (Fig. 4, left) When the reaction temperature is held at 80°C for one hour the silver is reduced at a rate of 0.028 mM Ag^+/minute, with complete reduction by 46 minutes (Fig. 4, right). These findings indicate that the temperature of the reaction has an impact on kinetic rates. Unfortunately, while the same kinetic investigation was attempted with the copper reaction the amount of copper present in the solution disappeared immediately upon reaction with the sodium bicarbonate, forming an insoluble copper (II) carbonate complex. The kinetic investigation could not be attempted for other synthesis methods due to the high pH of the reactions damaging the ISE.

While it was originally hypothesized that the effectiveness of $NaHCO_3$ for silver reduction was due to an optimal pH (pH = 8.24), it was identified that silver was still reduced at pH 6 (5400 ± 510 mg Ag/kg textile), pH 10 (8860 ± 1310 mg Ag/kg textile) and pH 12 (7500 ± 600 mg Ag/kg) (although reduction at pH 10 and 12 is likely due to the NaOH used to adjust the pH). The reduction at pH 6 indicates that the bicarbonate/carbonate ion itself has a key impact on the silver reduction. However, no reduction was found to occur at pH 3, indicating pH still plays a large role in the overall synthesis effectiveness (Figure S6).

3.2 Metal Particle Morphology

SEM analysis was performed on silver, copper, and bimetallic treated textiles resulting from the three synthesis methods that gave the most distinct results (Method 2, 5, 8). Initial SEM method development identified that most of the metal particles were present inside the cellulose matrix, requiring ashing of the textiles before analysis. To the author's knowledge this is the first study to identify metal materials present inside the cellulose matrix following in-situ synthesis. While classically defined nanoparticles (< 100 nm) were identified, the majority of the particles were found to be between 100 and 500 nm in diameter, which are considered nanomaterials depending on the application and field [7] (Fig. 5, 6).

For the bimetallic treated textiles, the combined presence of silver and copper particles precluded the measurement of the diameters, but visual examination of the SEM images and the corresponding EDX

spectra revealed two findings. Use of $NaHCO_3$ (Method 3) resulted in significantly more silver present than copper, whereas use of NaOH or $NaBH_4$ resulted in more copper present (predominantly green (copper) shading), which aligns with the XRF concentration results presented previously (Figure 6A). Secondly, the silver particles are significantly larger in the bimetallic textiles compared to silver only textiles, with many of them appearing to be well above 500 nm in diameter. Once again, this is likely caused by a lack of binding sites due to competition with the copper, causing the silver reduction to favor particle growth over new nanoparticle formation. The copper/ copper oxide nanoparticles are relatively unchanged in their diameters (based on visual inspection).

3.3 Role of Heat in Metal-Textile Synthesis

Previous studies have identified that increased temperatures result in increased reaction rates and chemical pathways possible during treatment of cellulose with metal salts [34].The role of heat was qualitatively investigated for silver, copper, and silver/copper treated textiles following treatment with $NaOH/NH_{3Version1}$. The synthesis was either performed at room temperature, with the solution heated after the textile was added, or the solution pre-heated (60°C) before adding the textile.

For silver an increase in heat results in an increase to the amount of silver reduced into the textile. For copper the textile color is different based on the heating profile. When the textile is added to the synthesis solution at room temperature the blue copper complex (copper-tetraammine-hydroxide) immediately binds to the cellulose, stabilizing it against thermal conversion to copper oxide (Fig. 7). The dark textile color corresponding to copper oxide only occurs when the solution is heated at 60°C before the textile is added. At higher pH (pH > 10) the expected copper complexes are either unstable or are not formed at elevated temperatures in water, resulting in the formation or conversion to copper oxide (Cudennec and Lecerf, 2003). Interestingly for the bimetallic textile the color of the textile resembles copper oxide containing textiles, suggesting a possible silver-copper complex is formed that results in the deposition of copper oxide. This indicates that at pH > 10 the competition between silver and copper could be both physical competition for binding sites and chemical competition for reagents.

3.4 Silver Copper Competition

The potential for competition between silver and copper was identified in the previous sections from XRF, XANES, and SEM analysis. To investigate this further, synthesis Method 6 ($NaOH/NH_{3Version1}$) was used to treat cotton textiles with different concentrations of silver and copper at a fixed (1:1) and variable ratio.

The relationship between the concentration of metal in the textile and in solution was plotted for silver, copper, and silver/copper treated textiles. The slope for the silver only synthesis was found to be 5600 mg Ag/kg textile per mM of reagent (introduced) Ag in solution (R^2 0.98). The slope for the copper only synthesis was found to be 2200 mg Cu/kg textile per mM of Cu in solution (R^2 0.95). For the silver synthesis in the combined silver/copper treatment, the slope for silver decreased dramatically to 240 mg Ag/kg textile per mM of Ag in solution (R^2 0.99), whereas for copper the slope barely decreased (2000 mg

Cu/kg textile per mM of Cu in solution, R^2 0.98) (Fig. 8). This confirms that, when silver and copper are in solution at equal concentrations, copper outcompetes silver for binding onto the textile.

Additionally, by varying the ratio of silver and copper (1:0, 10:1, 5:1, 2:1, 1:1, 0:1) the amount of copper required to outcompete silver can be identified. While the amount of silver decreased slightly with the addition of 0.1 and 0.2 mM of copper, it was within the deviation of the silver with no copper added. The amount of silver present on the textile dropped dramatically with 0.5 mM of copper being added, or a 2:1 ratio. Adding 1 mM of copper (1:1) resulted in further decrease in the amount of silver in the textile, indicating that copper began to significantly outcompete silver between a ratio of 5:1 and 2:1 (Fig. 8). This explains the dominant amount of silver compared to copper in Ag/Cu synthesis Method 2 ($NaHCO_3$), as this method showed to result in a large amount of silver but a small amount of copper, resulting in a silver/copper ratio of ~ 5:1 on the textile. Without any silver present, the amount of copper on the textile increased, indicating that while silver is disproportionately outcompeted by copper, the presence of silver does lead to some inhibition of copper binding to the textile. It is hypothesized that the stabilization of the copper oxide precipitate onto the textile occurs more rapidly than the reduction of silver, leading to the competition phenomena observed.

3.5 Cellulose Analysis

ATR-FTIR analysis was performed on samples treated with $NaOH/NH_{3Version1}$ (Method 6) with an increasing silver concentration (0.1–10 mM) to identify any changes to the cellulose structure following synthesis (Figure S12). Minor changes to various peak intensities were seen, thought to be due to differences in sample material thickness and homogeneity, and not actual changes to cellulose functional groups. The lack of identifiable functional group changes is expected when considering cellulose polymer chain length (degree of polymerization) for cotton is upwards of 10,000 units, and the reduction of silver only occurs at the termini of the polymer chain, leaving most of the cellulose untouched [31]. ATR-FTIR analysis of textiles resulting from Methods 2 ($NaHCO_3$),5 (NaOH), and 8 ($NaBH_4$) further confirm a lack of any functional group transformation (Fig. 9).

3.6 Parsimonious Assessment of the Synthesis Methods

The goal of this investigation was to identify the most parsimonious – successful, simple, and ideally, efficacious – method for creating silver and copper treated textiles by comparing novel and previously identified synthesis methods in a stepwise fashion. The effectiveness of the methods can be identified following comprehensive characterization of the concentration (highest), speciation (non-ionic) and morphology of metal (nanoparticulate) in the textiles.

For silver synthesis methods, treatment with $NaHCO_3$ or NaOH were assessed as the most parsimonious methods as they resulted in the highest concentrations of silver in the textile in metallic nanoparticulate form (100–500 nm). The use of ammonia, green tea, and $NaBH_4$ were all found to be ineffective as they reduce and/or stabilize the ionic silver in solution, inhibiting successful binding with the cellulose.

For synthesis of copper-treated textiles, Methods 4–8 were found to be comparable in their effectiveness, as they resulted in the highest concentrations of copper in the textile, forming nanoparticles (50–500 nm, with non-ionic copper speciation (i.e., copper oxide). Of the four methods, use of NaOH was the most parsimonious method as it resulted in the highest total concentration of copper with minimal reagent input.

For the bimetallic synthesis methods, the extent of metal on the textile was influenced by the competition between silver and copper for binding with the textile. The use of $NaHCO_3$ resulted in a parsimonious silver dominant synthesis method, resulting in a broad range of sizes in silver particles (greater than 1000 nm) interspersed with smaller (~ 50 to 300 nm) copper nanoparticles. The use of Methods 4–7 resulted in comparable amounts of copper oxide and metallic silver on the textile, with unreduced ionic silver also present. The use of either NH_3, NaOH, or $NaBH_4$ were identified as being the most parsimonious balanced silver/copper synthesis method, with $NaBH_4$ being slightly advantageous due to complete reduction of silver. However, this slight advantage is countered by the toxicity of using $NaBH_4$ as a reducing agent.

4. Conclusion

This study characterized silver, copper, and silver/copper containing cotton textiles resulting from eight different synthesis methods. The total metal content, metal speciation, and metal morphology of each synthesis reaction has been identified. Additionally, the roles of metal competition, temperature and pH (treatment with Ag/$NaHCO_3$) have also been investigated, providing additional mechanistic information.

A $NaHCO_3$ synthesis method (Method 2) resulted in the highest concentration (8900 ± 500 mg Ag/kg textile) of elemental silver nanoparticles (356 ± 106 nm) in the cotton textile material, representing a successful method for the creation of silver nanoparticle treated textiles. The NaOH synthesis method (Method 5) was also found to result in high concentrations of metallic (silver) and metal-oxide (copper) nanoparticles, representing a successful method for the creation of silver, copper, and bimetallic silver/copper containing textiles.

While the size of the nanoparticles identified in this study are larger than classically defined nanoparticles (< 100 nm in diameter), the larger size is potentially advantageous when considering their potential for antimicrobial textile applications. Larger-sized nanoparticles allow for sufficiently small particles to provide an enhanced ability (over sheets or coatings) to inhibit the growth of bacteria and viruses, while minimizing major nano-specific risk assessment concerns for the product [5, 7, 68]. The identification of the silver and copper materials being present inside the cellulose matrix suggests that the release of the metal materials during use and washing may be minimal. Future work is planned to evaluate the antimicrobial effectiveness of these silver, copper, and silver/copper treated textiles.

Declarations

ETHICS APPROVAL AND CONSENT TO PARTICIPATE

No ethics approval or consent to participate was required for this research.

CONSENT FOR PUBLICATION

All authors whose names appear on the submission have made substantial contributions to the publication, including but not limited to; conception, design, data acquisition, analysis, interpretation, writing, revisions, and have approved the version to be published. All authors agree to be accountable for all aspects of the work in ensuring that questions related to the accuracy or integrity of any part of the work are appropriately investigated and resolved.

AVAILABILITY OF DATA AND MATERIALS

The data that support the findings of this study are available from the corresponding author upon reasonable request.

COMPETING INTERESTS

The authors have no financial or non-financial interests that could impart bias on the work submitted for publication.

FUNDING

This research was supported by Natural Sciences and Engineering Research Council of Canada Discovery Grants held by Koch and Weber.

AUTHORS' CONTRIBUTIONS

Conceptualization: David Patch, Kela Weber, Iris Koch; Methodology: David Patch; Formal analysis and investigation: David Patch, Natalia O'Connor, Debora Meira; Writing – original draft preparation: David Patch; Writing- review and editing: Natalia O'Connor, Iris Koch, Jennifer Scott, Kela Weber; Funding acquisition: Kela Weber; Resources: Iris Koch, Jennifer Scott, Kela Weber; Supervision: Iris Koch, Jennifer Scott, Kela Weber.

ACKNOWLEDGEMENTS

The authors would like to acknowledge Jacob Zachariah, Angela Richard and Francesca Body for their contributions to the initial literature review. The authors would like to acknowledge Brigitte Simmatis and Anbareen Farooq for their contributions with proofreading. The authors would also like to thank Dr. Jennifer Snelgrove for training and assistance with the SEM-EDX work, Dr. Fiona Kelly for providing her NexION 300D ICP-MS, as well as Dr. Zou Finfrock for performing XANES speciation analysis. This research used resources of the Advanced Photon Source, an Office of Science User Facility operated for the U.S. Department of Energy (DOE) Office of Science by Argonne National Laboratory and was supported by the U.S. DOE under Contract No. DE- AC02-06CH11357, the Canadian Light Source and its

funding partners (Sector 20 work), and DOE and MRCAT member institutions (Sector ID-B). Additional beam time was awarded for research related to COVID applications.

References

1. Nowack, B., Krug, H.F., and Height, M. (2011) 120 years of nanosilver history: Implications for policy makers. *Environmental Science and Technology*.
2. Giannossa, L.C., Longano, D., Ditaranto, N., Nitti, M.A., Paladini, F., Pollini, M., Rai, M., Sannino, A., Valentini, A., and Cioffi, N. (2013) Metal nanoantimicrobials for textile applications. *Nanotechnology Reviews*, **2** (3), 307–331.
3. Alexander, J.W. (2009) History of the medical use of silver. *Surg Infect (Larchmt)*, **10** (3), 289–292.
4. Fernández, J.G., Fernández-Baldo, M.A., Berni, E., Camí, G., Durán, N., Raba, J., and Sanz, M.I. (2016) Production of silver nanoparticles using yeasts and evaluation of their antifungal activity against phytopathogenic fungi. *Process Biochemistry*, **51** (9), 1306–1313.
5. Health, N.I. (2010) Risks Scientific Basis for the Definition of the Term " Nanomaterial ." (July), 1–43.
6. Drexler, E. (1986) The coming era of nanotechnology.
7. Gubala, V., Johnston, L.J., Liu, Z., Krug, H., Moore, C.J., Ober, C.K., Schwenk, M., and Vert, M. (2018) Engineered nanomaterials and human health: Part 1. Preparation, functionalization and characterization (IUPAC Technical Report). *Pure and Applied Chemistry*, **90** (8), 1283–1324.
8. Idumah, C.I. (2021) Influence of nanotechnology in polymeric textiles, applications, and fight against COVID-19. *Journal of the Textile Institute*, **112** (12), 2056–2076.
9. Gasana, E., Westbroek, P., Hakuzimana, J., de Clerck, K., Priniotakis, G., Kiekens, P., and Tseles, D. (2006) Electroconductive textile structures through electroless deposition of polypyrrole and copper at polyaramide surfaces. *Surface and Coatings Technology*, **201** (6), 3547–3551.
10. Root, W., Aguiló-Aguayo, N., Pham, T., and Bechtold, T. (2018) Conductive layers through electroless deposition of copper on woven cellulose lyocell fabrics. *Surface and Coatings Technology*, **348** (April), 13–21.
11. Allahyarzadeh, V., Montazer, M., Nejad, N.H., and Samadi, N. (2013) In situ synthesis of nano silver on polyester using NaOH/Nano TiO 2. *Journal of Applied Polymer Science*, **129** (2), 892–900.
12. Lu, Y., Jiang, S., and Huang, Y. (2010) Ultrasonic-assisted electroless deposition of Ag on PET fabric with low silver content for EMI shielding. *Surface and Coatings Technology*, **204** (16–17), 2829–2833.
13. Shateri-Khalilabad, M., Yazdanshenas, M.E., and Etemadifar, A. (2017) Fabricating multifunctional silver nanoparticles-coated cotton fabric. *Arabian Journal of Chemistry*, **10**, S2355–S2362.
14. Hasan, R. (2018) Production of Antimicrobial Textiles by Using Copper Oxide Nanoparticles. *International Journal of Contemporary Research and Review*, **9** (08), 20195–20202.
15. Üreyen, M.E., Doğan, A., and Koparal, A.S. (2012) Antibacterial functionalization of cotton and polyester fabrics with a finishing agent based on silver-doped calcium phosphate powders. *Textile*

Research Journal, **82** (17), 1731–1742.

16. Rajendra, R., Balakumar, C., Ahammed, H., Jayakumar, S., Vaideki, K., and Rajesh, E. (2010) Use of zinc oxide nano particles for production of antimicrobial textiles. *International Journal of Engineering, Science and Technology*, **2** (1), 202–208.
17. Ditaranto, N., Picca, R.A., Sportelli, M.C., Sabbatini, L., and Cioffi, N. (2016) Surface characterization of textiles modified by copper and zinc oxide nano-antimicrobials. *Surface and Interface Analysis*, **48** (7), 505–508.
18. Cheng, T.H., Yang, Z.Y., Tang, R.C., and Zhai, A.D. (2020) Functionalization of silk by silver nanoparticles synthesized using the aqueous extract from tea stem waste. *Journal of Materials Research and Technology*, **9** (3), 4538–4549.
19. Gaikwad, S., Ingle, A., Gade, A., Rai, M., Falanga, A., Incoronato, N., Russo, L., Galdiero, S., and Galdiero, M. (2013) Antiviral activity of mycosynthesized silver nanoparticles against herpes simplex virus and human parainfluenza virus type 3. *International Journal of Nanomedicine*, **8**, 4303–4314.
20. Cuevas, R., Durán, N., Diez, M.C., Tortella, G.R., and Rubilar, O. (2015) Extracellular biosynthesis of copper and copper oxide nanoparticles by Stereum hirsutum, a native white-rot fungus from chilean forests. *Journal of Nanomaterials*, **2015**.
21. El-Rafie, H.M., El-Rafie, M.H., and Zahran, M.K. (2013) Green synthesis of silver nanoparticles using polysaccharides extracted from marine macro algae. *Carbohydrate Polymers*, **96** (2), 403–410.
22. Root, W., Aguiló-Aguayo, N., Pham, T., and Bechtold, T. (2018) Conductive layers through electroless deposition of copper on woven cellulose lyocell fabrics. *Surface and Coatings Technology*, **348** (May), 13–21.
23. Chen, H., Liao, F., Yuan, Z., Han, X., and Xu, C. (2017) Simple and fast fabrication of conductive silver coatings on carbon fabrics via an electroless plating technique. *Materials Letters*, **196**, 205–208.
24. Srikar, S.K., Giri, D.D., Pal, D.B., Mishra, P.K., and Upadhyay, S.N. (2016) Green Synthesis of Silver Nanoparticles: A Review. Green and Sustainable Chemistry. *Green and Sustainable Chemistry*, **6** (February), 34–56.
25. Rafique, M., Sadaf, I., Rafique, M.S., and Tahir, M.B. (2017) A review on green synthesis of silver nanoparticles and their applications. *Artificial Cells, Nanomedicine and Biotechnology*, **45** (7), 1272–1291.
26. Vigneshwaran, N., Nachane, R.P., Balasubramanya, R.H., and Varadarajan, P. v. (2006) A novel one-pot “green” synthesis of stable silver nanoparticles using soluble starch. *Carbohydrate Research*, **341** (12), 2012–2018.
27. Maryan, A.S., Montazer, M., and Harifi, T. (2015) Synthesis of nano silver on cellulosic denim fabric producing yellow colored garment with antibacterial properties. *Carbohydrate Polymers*, **115**, 568–574.
28. Montazer, M., and Allahyarzadeh, V. (2013) Electroless plating of silver nanoparticles/nanolayer on polyester fabric using AgNO3/NaOH and ammonia. *Industrial and Engineering Chemistry Research*, **52** (25), 8436–8444.

29. Allahyarzadeh, V., Montazer, M., Nejad, N.H., and Samadi, N. (2013) In situ synthesis of nano silver on polyester using NaOH/Nano TiO 2. *Journal of Applied Polymer Science*, **129** (2), 892–900.
30. Miyamoto, T., Takahashi, S. -i, Ito, H., Inagaki, H., and Noishiki, Y. (1989) Tissue biocompatibility of cellulose and its derivatives. *Journal of Biomedical Materials Research*, **23** (1), 125–133.
31. Klemm, D., Heublein, B., Fink, H.P., and Bohn, A. (2005) Cellulose: Fascinating biopolymer and sustainable raw material. *Angewandte Chemie - International Edition*, **44** (22), 3358–3393.
32. Peng, H., Liu, Y., Peng, W., Zhang, J., and Ruan, R. (2016) Green synthesis and stability evaluation of Ag nanoparticles using bamboo hemicellulose. *BioResources*, **11** (1), 385–399.
33. Xu, Q., Ke, X., Ge, N., Shen, L., Zhang, Y., Fu, F., and Liu, X. (2018) Preparation of Copper Nanoparticles Coated Cotton Fabrics with Durable Antibacterial Properties. *Fibers and Polymers*, **19** (5), 1004–1013.
34. Jiang, T., Liu, L., and Yao, J. (2011) In situ deposition of silver nanoparticles on the cotton fabrics. *Fibers and Polymers*, **12** (5), 620–625.
35. Zhang, S., Tang, Y., and Vlahovic, B. (2016) A Review on Preparation and Applications of Silver-Containing Nanofibers. *Nanoscale Research Letters*, **11** (1), 1–8.
36. Sun, Q., Cai, X., Li, J., Zheng, M., Chen, Z., and Yu, C.P. (2014) Green synthesis of silver nanoparticles using tea leaf extract and evaluation of their stability and antibacterial activity. *Colloids and Surfaces A: Physicochemical and Engineering Aspects*, **444**, 226–231.
37. Gagnon, V., Button, M., Boparai, H.K., Nearing, M., O'Carroll, D.M., and Weber, K.P. (2019) Influence of realistic wearing on the morphology and release of silver nanomaterials from textiles. *Environmental Science: Nano*.
38. Benn, T.M., and Westerhoff, P. (2008) Nanoparticle silver released into water from commercially available sock fabrics. *Environmental Science and Technology*, **42** (11), 4133–4139.
39. Tang, B., Kaur, J., Sun, L., and Wang, X. (2013) Multifunctionalization of cotton through in situ green synthesis of silver nanoparticles. *Cellulose*, **20** (6), 3053–3065.
40. Yuen, C.W.M., Jiang, S.X., Kan, C.W., Ku, S.K.A., Choi, P.S.R., Tang, K.P.M., and Cheng, S.Y. (2013) Polyester metallisation with electroless silver plating process. *Fibers and Polymers*, **14** (1), 82–88.
41. Liu, B., Li, X., Zheng, C., Wang, X., and Sun, R. (2013) Facile and green synthesis of silver nanoparticles in quaternized carboxymethyl chitosan solution. *Nanotechnology*, **24** (23).
42. Montazer, M., Alimohammadi, F., Shamei, A., and Rahimi, M.K. (2012) In situ synthesis of nano silver on cotton using Tollens' reagent. *Carbohydrate Polymers*, **87** (2), 1706–1712.
43. Kongruang, S., Han, M.J., Breton, C.I.G., and Penner, M.H. (2004) Quantitative analysis of cellulose-reducing ends. *Applied Biochemistry and Biotechnology - Part A Enzyme Engineering and Biotechnology*, **113** (1–3), 213–231.
44. Matsuoka, S., Kawamoto, H., and Saka, S. (2011) Reducing end-group of cellulose as a reactive site for thermal discoloration. *Polymer Degradation and Stability*, **96** (7), 1242–1247.

45. Haskins, J., and Hogsed, M. (1950) THE ALKALINE OXIDATION OF CELLULOSE. I. MECHANISM OF THE DEGRADATIVE OXIDATION OF CELLULOSE BY HYDROGEN PEROXIDE IN PRESENCE OF ALKALI. 1264–1274.
46. van Loon, L.R., and Glaus, M.A. (1998) Experimental and Theoretical Studies on Alkaline Degradation of Cellulose and its Impact on the Sorption of Radionuclides. **37** (4), 2002.
47. Zahran, M.K., Ahmed, H.B., and El-Rafie, M.H. (2014) Facile size-regulated synthesis of silver nanoparticles using pectin. *Carbohydrate Polymers*, **111**, 971–978.
48. Peng, H., Wang, N., Zhang, J., and Yu, Z. (2011) Synthesis of silver nanoparticles by using bamboo hemicellulose as template in aqueous solution. *Advanced Materials Research*, **311–313**, 149–154.
49. Sadanand, V., Tian, H., Rajulu, A.V., and Satyanarayana, B. (2017) Antibacterial cotton fabric with in situ generated silver nanoparticles by one-step hydrothermal method. *International Journal of Polymer Analysis and Characterization*, **22** (3), 275–279.
50. Biedermen, G., and Sillen, L.G. (1960) Studies on the Hydrolysis of Metal Ions. Part 30. A Critical Survey on the Solubility Equilibria of Ag2O. 9.
51. Garza-Navarro, M.A., Aguirre-Rosales, J.A., Llanas-Vázquez, E.E., Moreno-Cortez, I.E., Torres-Castro, A., and González-González, V. (2013) Totally ecofriendly synthesis of silver nanoparticles from aqueous dissolutions of polysaccharides. *International Journal of Polymer Science*, **2013** (Cmc).
52. Hebeish, A.A., El-Rafie, M.H., Abdel-Mohdy, F.A., Abdel-Halim, E.S., and Emam, H.E. (2010) Carboxymethyl cellulose for green synthesis and stabilization of silver nanoparticles. *Carbohydrate Polymers*, **82** (3), 933–941.
53. Onitsuka, S., Hamada, T., and Okamura, H. (2019) Preparation of antimicrobial gold and silver nanoparticles from tea leaf extracts. *Colloids and Surfaces B: Biointerfaces*, **173**, 242–248.
54. Asghar, M.A., Zahir, E., Shahid, S.M., Khan, M.N., Asghar, M.A., Iqbal, J., and Walker, G. (2018) Iron, copper and silver nanoparticles: Green synthesis using green and black tea leaves extracts and evaluation of antibacterial, antifungal and aflatoxin B1 adsorption activity. *LWT - Food Science and Technology*, **90** (December 2017), 98–107.
55. Rónavári, A., Kovács, D., Igaz, N., Vágvölgyi, C., Boros, I.M., Kónya, Z., Pfeiffer, I., and Kiricsi, M. (2017) Biological activity of green-synthesized silver nanoparticles depends on the applied natural extracts: A comprehensive study. *International Journal of Nanomedicine*, **12**, 871–883.
56. Sun, Q., Cai, X., Li, J., Zheng, M., Chen, Z., and Yu, C.P. (2014) Green synthesis of silver nanoparticles using tea leaf extract and evaluation of their stability and antibacterial activity. *Colloids and Surfaces A: Physicochemical and Engineering Aspects*, **444**, 226–231.
57. Arumai Selvan, D., Mahendiran, D., Senthil Kumar, R., and Kalilur Rahiman, A. (2018) Garlic, green tea and turmeric extracts-mediated green synthesis of silver nanoparticles: Phytochemical, antioxidant and in vitro cytotoxicity studies. *Journal of Photochemistry and Photobiology B: Biology*, **180** (2017), 243–252.
58. Ahmad, S., Munir, S., Zeb, N., Ullah, A., Khan, B., Ali, J., Bilal, M., Omer, M., Alamzeb, M., Salman, S.M., and Ali, S. (2019) Green nanotechnology: A review on green synthesis of silver nanoparticles — An

ecofriendly approach. *International Journal of Nanomedicine*, **14**, 5087–5107.

59. Polte, J., Tuaev, X., Wuithschick, M., Fischer, A., Thuenemann, A.F., Rademann, K., Kraehnert, R., and Emmerling, F. (2012) Formation mechanism of colloidal silver nanoparticles: Analogies and differences to the growth of gold nanoparticles. *ACS Nano*, **6** (7), 5791–5802.
60. Glavee, G.N., Klabunde, K.J., Sorensen, C.M., and Hadjipanayis, G.C. (1995) Chemistry of borohydride reduction of iron(II) and iron(III) ions in aqueous and nonaque-ous media. *Inorganic Chemistry*, **34** (1), 28–35.
61. Glavee, G.N., Klabunde, K.J., Sorensen, C.M., and Hadjipanayis, G.C. (1994) Borohydride Reduction of Nickel and Copper Ions in Aqueous and Nonaqueous Media. Controllable Chemistry Leading to Nanoscale Metal and Metal Boride Particles. *Langmuir*, **10** (12), 4726–4730.
62. Wojtysiak, S., and Kudelski, A. (2012) Influence of oxygen on the process of formation of silver nanoparticles during citrate/borohydride synthesis of silver sols. *Colloids and Surfaces A: Physicochemical and Engineering Aspects*, **410**, 45–51.
63. Noordeen, S., Karthikeyan, K., and Parveen, M. a N. (2013) Synthesis of Silver Nanoparticles by using Sodium Borohydride as a Reducing Agent. *International Journal of Engineering Research and Technology*, **2** (4), 388–397.
64. Dong, X., Ji, X., Jing, J., Li, M., Li, J., and Yang, W. (2010) Synthesis of triangular silver nanoprisms by stepwise reduction of sodium borohydride and trisodium citrate. *Journal of Physical Chemistry C*, **114** (5), 2070–2074.
65. Hyning, D.L. van, and Zukoski, C.F. (1998) Formation Mechanisms and Aggregation Behavior of Borohydride Reduced Silver Particles. *Langmuir*, (20), 7034–7046.
66. Glavee, G.N., Klabunde, K.J., Sorensen, C.M., and Hadjapanayis, G.C. (1992) Borohydride Reductions of Metal Ions. A New Understanding of the Chemistry Leading to Nanoscale Particles of Metals, Borides, and Metal Borates. *Langmuir*, (8), 771–773.
67. Cudennec, Y., and Lecerf, A. (2003) The transformation of Cu(OH)2 into CuO, revisited. *Solid State Sciences*, **5** (11–12), 1471–1474.
68. Ray, P.C., Yu, H., and Fu, P.P. (2009) Toxicity and environmental risks of nanomaterials: challenges and future needs. *J Environ Sci Health C Environ Carcinog Ecotoxicol Rev*, **27** (1), 1–35.

Figures

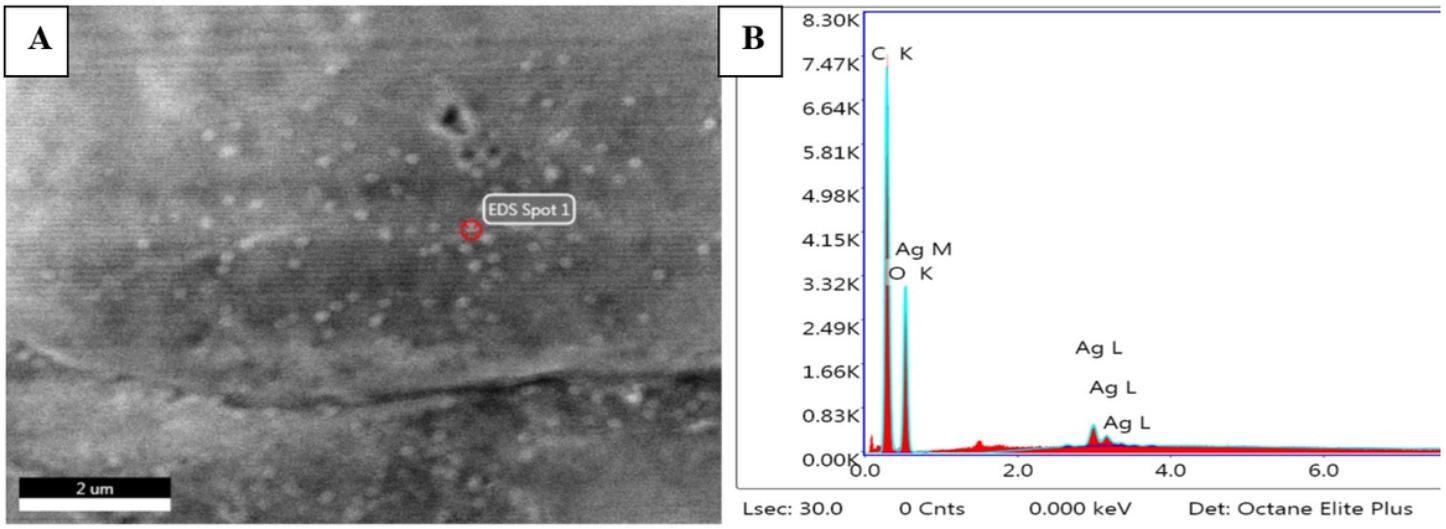

Figure 1

Silver nanoparticles found in the cross-section of the cotton fiber following $NaHCO_3$ silver treatment method.

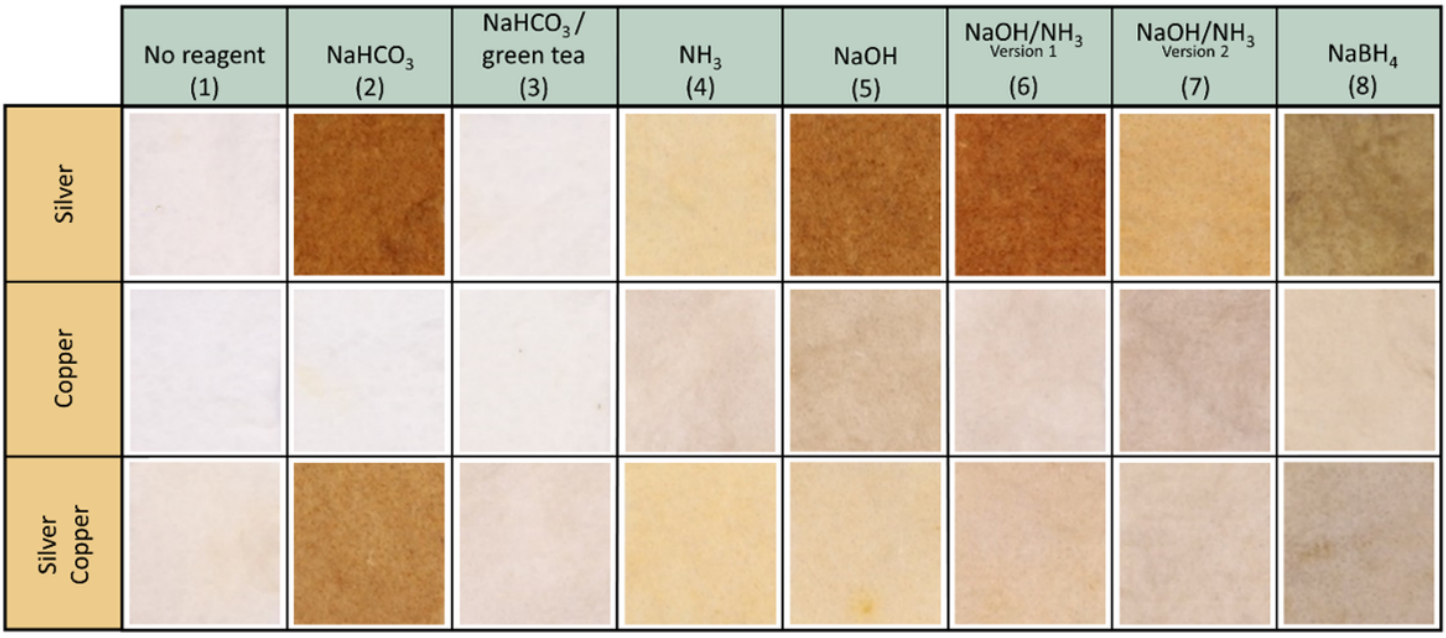

Figure 2

Photographic images taken of finished textiles using eight synthesis methods.

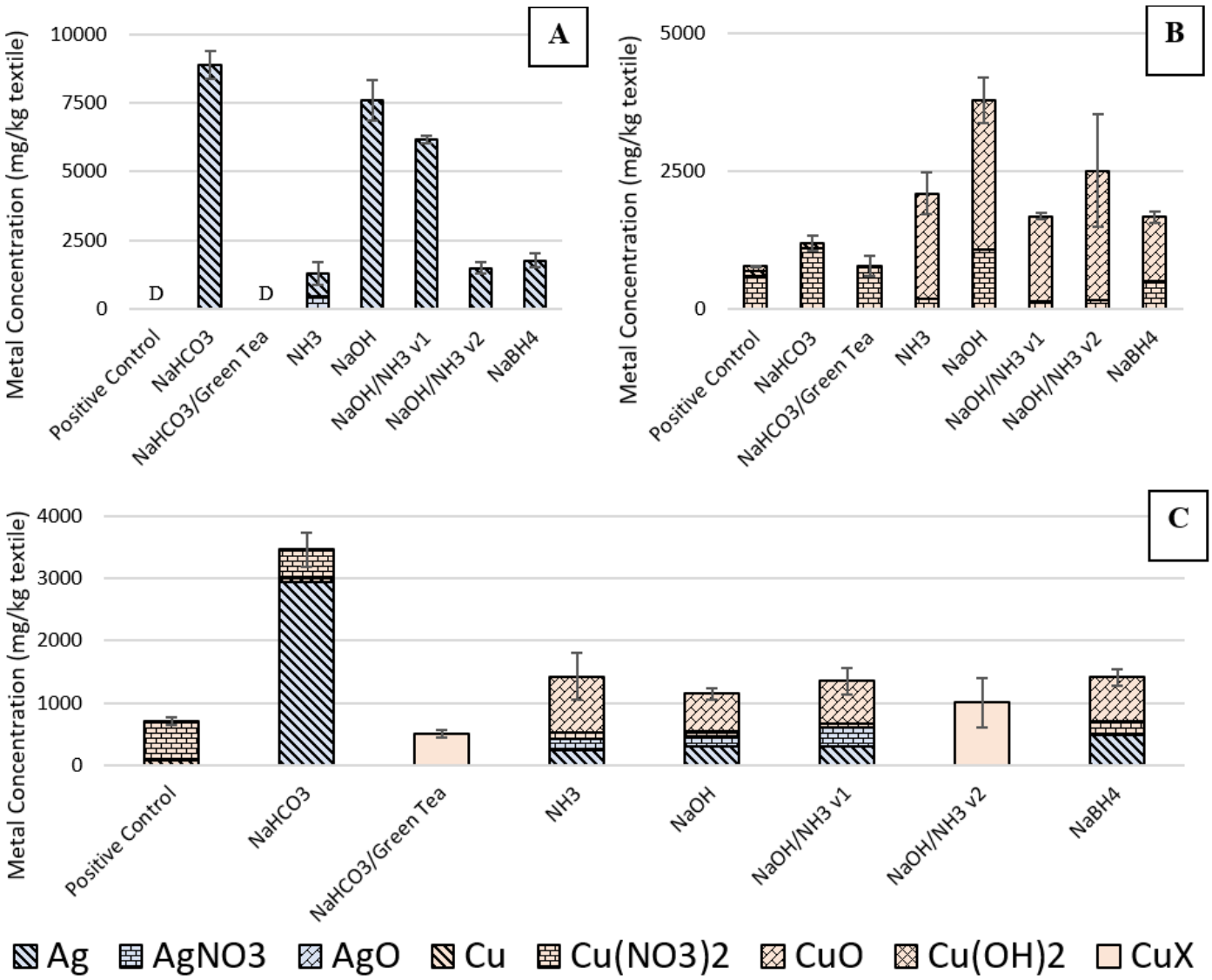

Figure 3

Concentration of metal present in the textile following treatment with (A) 1mM silver, (B) 1mM copper, and (C) combined 0.5 mM/0.5 mM silver/copper using XRF. Speciation information was obtained from XANES. CuX are samples that do not have speciation data available. D are samples that were not detected by XRF but have speciation data available. Error bars are the standard deviation of triplicate.

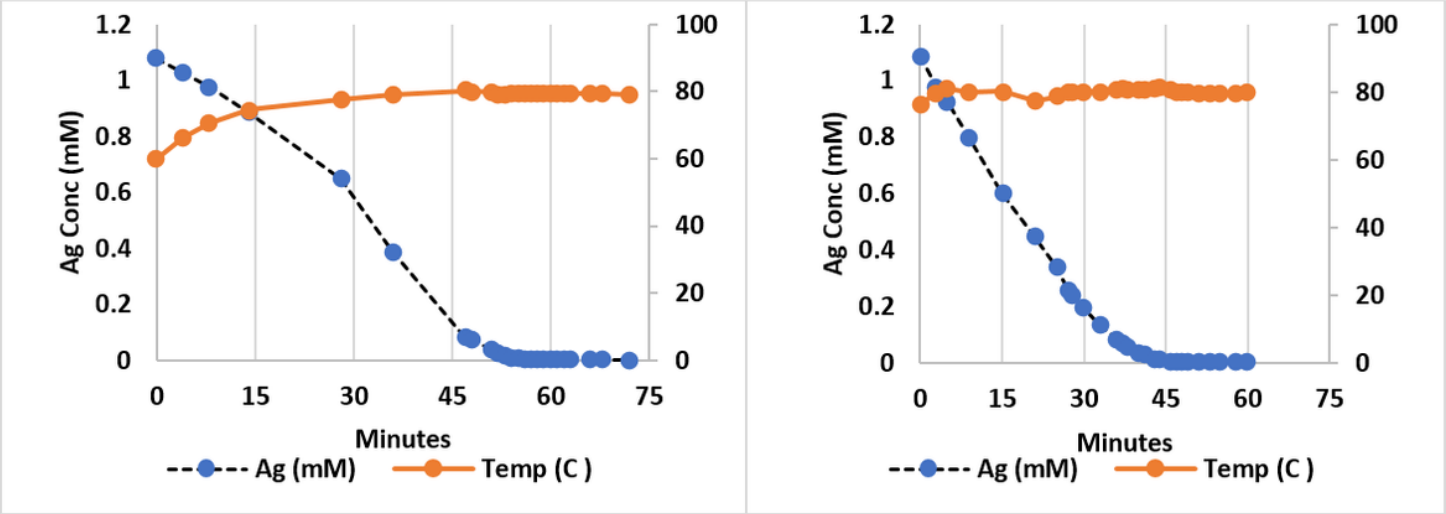

Figure 4

In-situ silver ion selective electrode measurements examining the rate of reaction at two different temperature profiles following $NaHCO_3$ synthesis method.

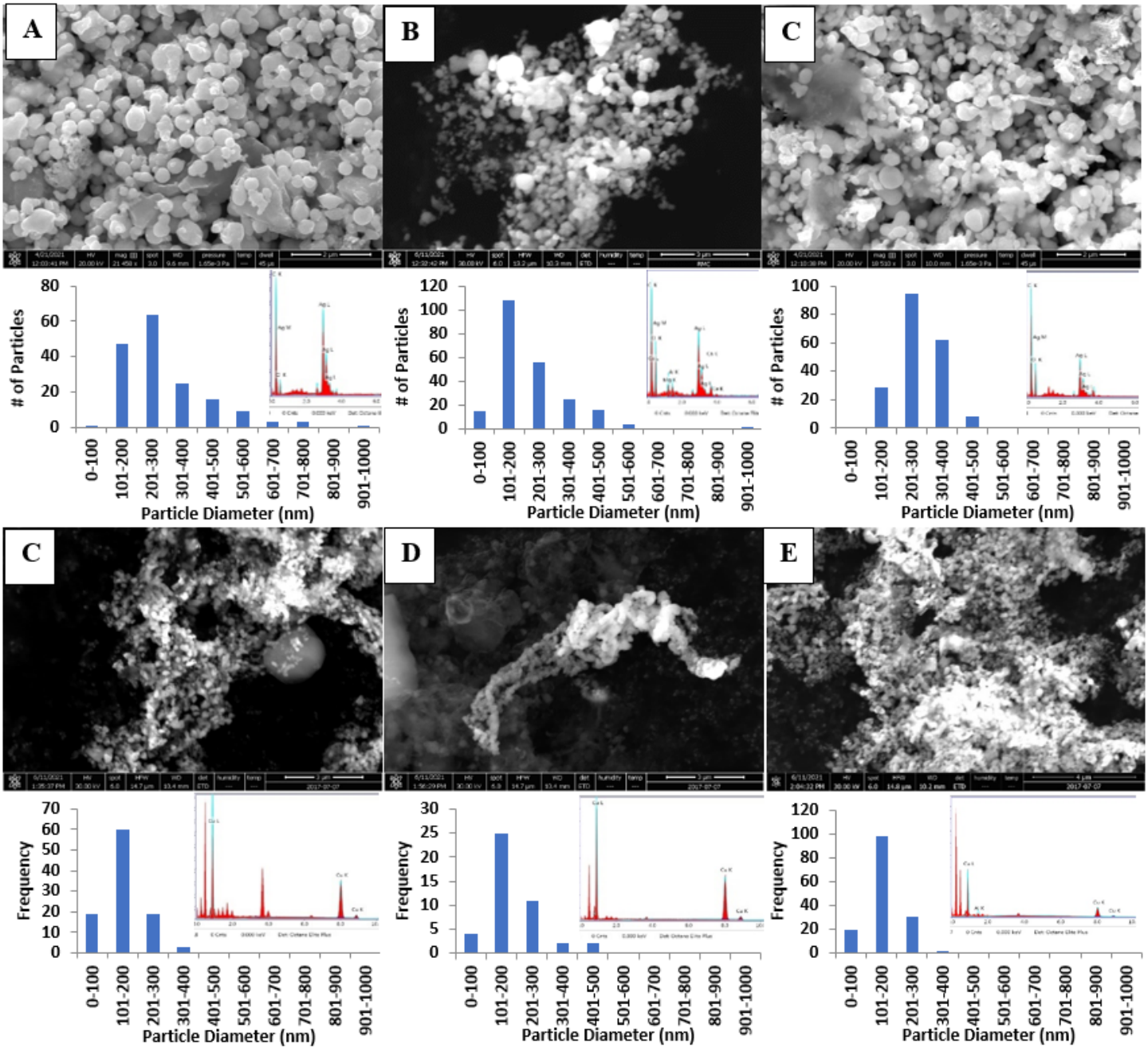

Figure 5

SEM analysis, EDX spectra, and ImageJ particle number/diameter determination of silver nanomaterials (A-C) and copper oxide nanomaterials (C-E) using $NaHCO_3$ (A/C), NaOH (B/D), and $NaBH_4$ (C/E) synthesis methods.

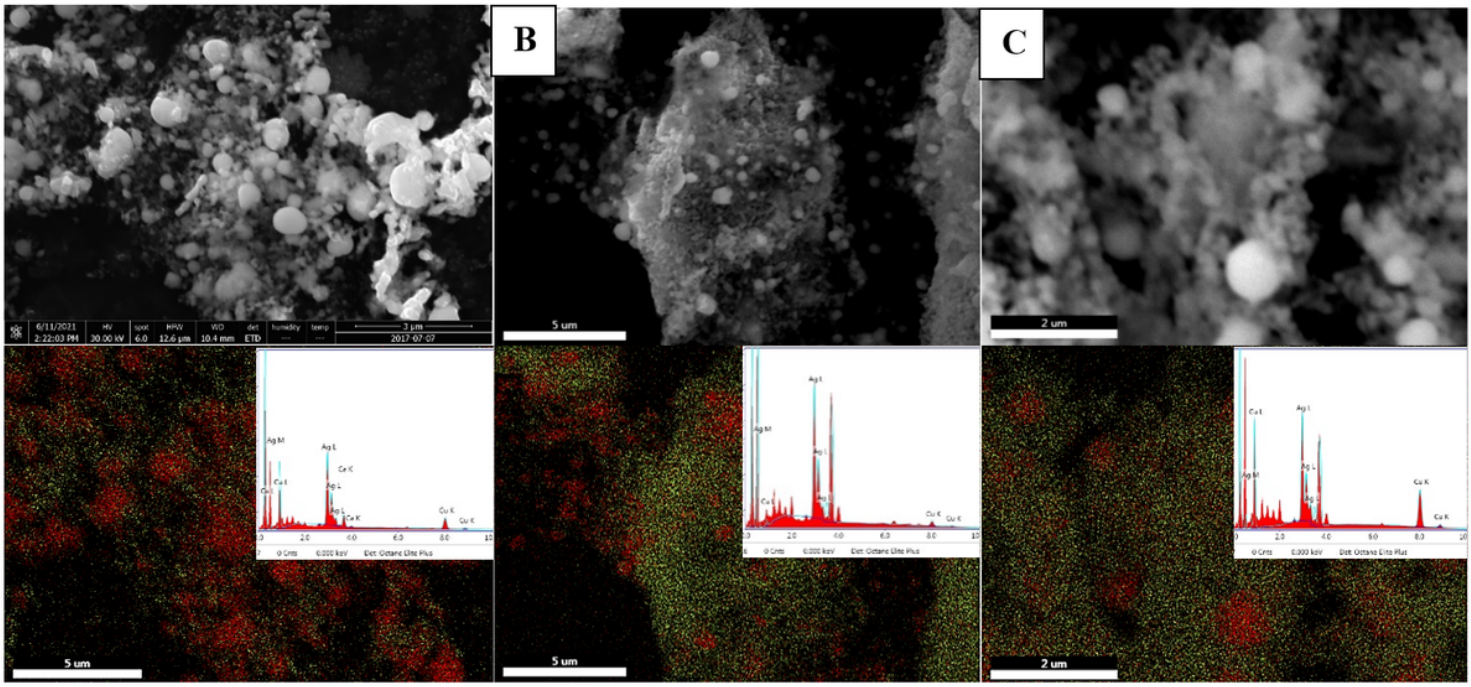

Figure 6

SEM analysis (top) and EDX elemental analysis (bottom) on silver (red) and copper (green) nanomaterials following $NaHCO_3$ (A), NaOH (B), and $NaBH_4$ (C) synthesis methods.

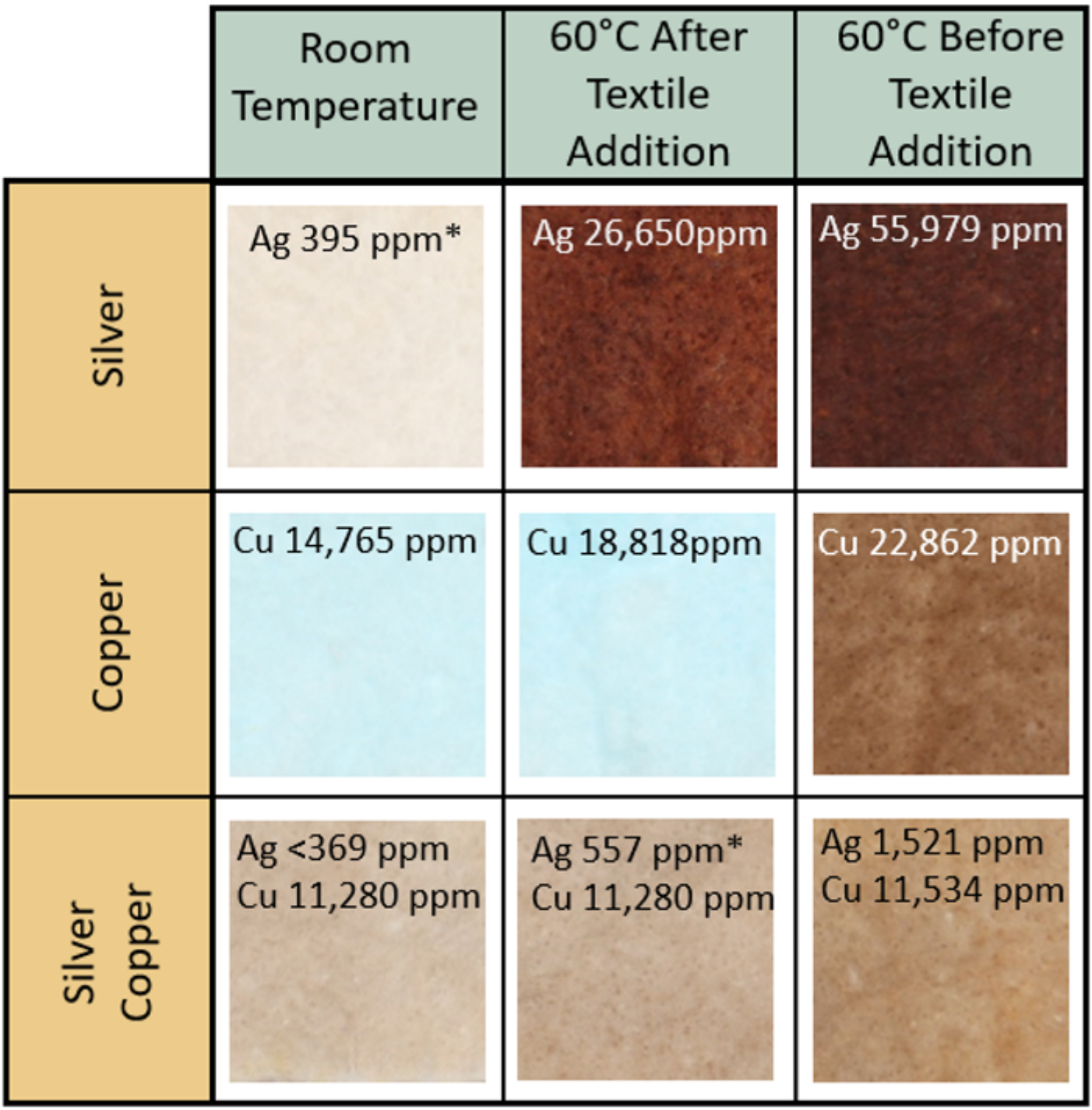

Figure 7

Pohotographic images of the synthesis of silver, copper, and silver/copper treated cotton textiles with three different water bath heat treatments using the $NaOH/NH_{3\ Version\ 1}$ synthesis method and 10 mM of starting metal concentration. Starred values have one replicate under XRF detection limits.

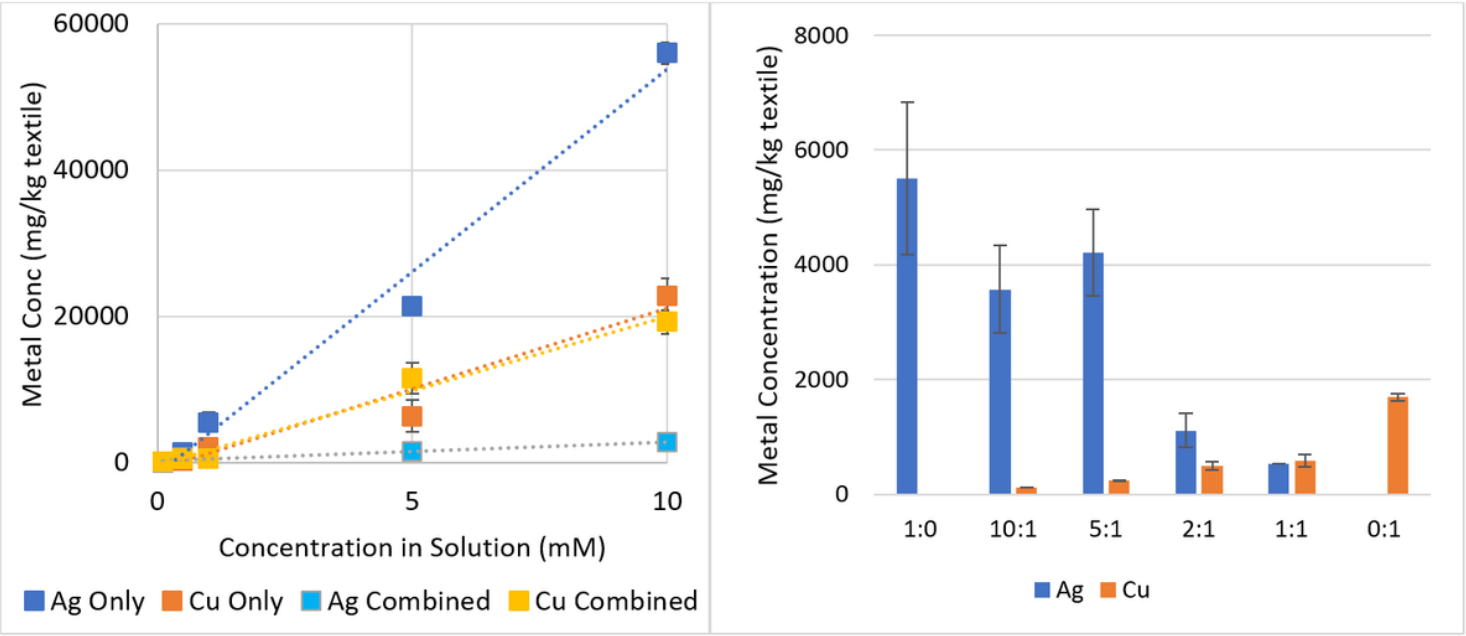

Figure 8

Investigation into the effect of reagent concentration on resulting concentration in the textile using the $NaOH/NH_{3Version1}$ synthesis method by using a fixed ratio of silver/copper (left) and a variable ratio of silver:copper, with silver held constant at 1 mM (except for 0:1, which had no silver and 1 mM copper) (right).

Supplementary Files

This is a list of supplementary files associated with this preprint. Click to download.

- DavidPatchTextileSIKPW.docx
- GraphicaAbstarct.png